IEEE Access
Multidisciplinary | Rapid Review | Open Access Journal

Received August 8, 2019, accepted September 2, 2019, date of publication September 5, 2019, date of current version September 23, 2019.

Digital Object Identifier 10.1109/ACCESS.2019.2939594

Receiver-Oriented Spatial Modulation in Visible Light Communication System

MANH LE TRAN AND SUNGHWAN KIM
School of Electrical Engineering, University of Ulsan, Ulsan 44610, South Korea
Corresponding author: Sunghwan Kim (sungkim@ulsan.ac.kr)

This work was supported by the Research Program through the National Research Foundation of Korea under Grant NRF-2016R1D1A1B03934653 and Grant NRF-2019R1A2C1005920.

ABSTRACT In this paper, we propose a receiver orientation model for spatial modulation (SM) in a visible light communication (VLC) system with line-of-sight (LOS) characteristics. The proposed technique efficiently mitigates the optical channel correlations across the multiple light-emitting diodes (LEDs), which are utilized in the SM system transmitter by altering the orientations of a photodiode (PD). Specifically, we express the LOS channel coefficients in the form of a PD normal vector and solve the optimization problems to obtain the optimal PD normal vectors. The bit error rate (BER) and channel capacity performances are also presented to validate the advantages of the proposed methods. The results demonstrate that the proposed designs offer a relatively low BER and high channel capacity in various LOS locations.

INDEX TERMS Visible light communications (VLC), spatial modulation (SM), maximum likelihood (ML) detection, convex optimization.

I. INTRODUCTION

Recently, there has been steadily increasing interest in visible light communication (VLC) as a very promising solution for indoor high-speed data transmission [1], [2]. Owing to the integration of communication and lighting features, VLC has been regarded as a complementary technique for future wireless networks, especially in indoor environments. For VLC, the modulated signal must be real-valued and non-negative, which is different from traditional radio frequency communication systems. Moreover, intensity modulation and direct detection techniques have been generally employed at the transmitter and receiver in the VLC system [3].

In a general indoor environment, multiple light-emitting diode (LED) sources are popularly utilized to provide for illumination [3]. Therefore, multiple-input multiple-output (MIMO) has been a popular technique that has been employed and investigated in VLC systems. However, due to the strong correlation property of the indoor MIMO VLC channel matrix, the shape of the receiver arrays must be specifically designed or the size of the array has to be several decimeters in length to achieve a full-rank channel matrix [4]. On the other hand, the multiple-input single-output (MISO) technique has also been a suitable option for various indoor VLC scenarios [5]–[7].

The increase in degrees of freedom provided by the availability of multiple LEDs as transmitters can be exploited to offer communication links at remarkable data rates [1]. Recently, various modulation schemes have been considered for both MIMO and MISO indoor optical wireless communication systems. For example, spatial multiplexing was a well-known concept that enhances the spectral efficiency of the system by simultaneously transmitting different data signals from multiple LEDs [8]. Furthermore, space shift keying (SSK) has been considered in VLC systems, which allows only one active LED at one time to limit inter-channel interference and support a high data rate with low-complexity detection [9]. Spatial modulation (SM) has been proposed, which is a combined MIMO and pulse amplitude modulation (PAM) technique that adds the spatial dimension to the constellation diagram. Specifically, an LED was activated at one time to transmit a PAM symbol, with a consequent increase in the overall system spectral efficiency [10], [11].

On the other hand, owing to the highly directional characteristics of light propagation through VLC channels, the communication through VLC channels has mainly relied on the availability of line-of-sight (LOS) links [3]. The orientation and mobility of the receiver are the two most important

The associate editor coordinating the review of this manuscript and approving it for publication was Zhenhui Yuan.

factors that affect the quality of the LOS links in VLC [12]. Due to the field of view (FOV) of the photodiode (PD), the direct influence of the PD orientation on the existence and the signal quality of LOS links becomes even more significant. This is particularly true because the correlation between the channel coefficients is an important factor that greatly impacts the performance of VLC systems [13]. Recently, the effect of the PD orientation and mobility on VLC systems has been greatly discussed in various studies [12], [14]–[17]. More specifically, the received signal strength is significantly affected by the angle between the arrival direction of the LOS signal and the PD normal vector. This incidence angle can be conveniently modified by directly changing the orientation of the receiver [12]. As a solution, utilization of the angle diversity receivers has been proposed in [14] to consider the employment of multiple PDs with different inclination angles on small mobile devices. In [14], the receiver employed several PDs with different orientation vectors that are arranged in a well-defined structure. However, the design in [14] required a specific structure of the receiver and a defined arrangement of the PDs on the receiver. Consequently, this brought about some issues when designing the receiver in a MIMO VLC system and these conditions further reduce the flexibility of the receiver in practical scenarios. Even though consideration of a receiver with several PDs oriented in different directions has already been considered, there is not much research on PD orientations in the VLC system.

In this paper, we propose a novel solution for improving the performance of SM VLC systems by altering the orientation of the PD. It is well-known that the performance of a VLC system can be evaluated using the bit error rate performance (BER). On the other hand, the channel capacity is also a popular measurement for the performance of the VLC channel. In particular, we address the problem of designing the normal vector of the PD that solve the minimum Euclidean distance (ED) and the maximum channel capacity problems. Specifically, the channel matrix coefficients of a VLC system can be expressed as the function of the PD orientation parameters or normal vectors of the PD. By considering the effect of PD orientation when constructing the optimization problems and by solving the convex optimization problems using different techniques, solutions for improving the SM VLC system performance can be achieved in the form of PD normal vectors. Consequently, the normal vectors for the PD can be obtained and utilized as the additional information in the setup and design of practical SM VLC systems. The simulation results show that the proposed algorithms can have good performance in both the channel capacity and BER over various receiver locations and are practical solutions to enable VLC transmission.

The rest of this paper is organized as follows. In Section II, we describe the system model and the normal vector of the PD, which is critical for the optimized orientation of the PD. The improved BER performance by altering the normal vector of the PD is detailed in Section III. In Section IV, the algorithm for improving the channel capacity is presented.

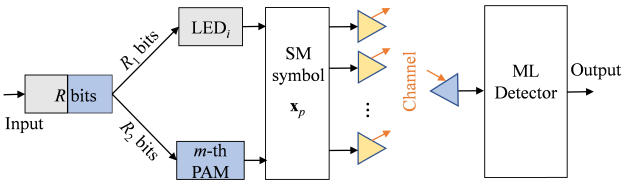

FIGURE 1. SM VLC system.

The performances of the two proposed solutions are analyzed in section V, including the BER performance and the channel capacity. Finally, we offer our conclusions in Section VI.

Notations: We use bold lower- and upper-case letters for column vectors and matrices, respectively. For a vector $\mathbf{a}$, a_i denotes its i-th element. For a matrix $\mathbf{A}$, $\mathbf{A}_{mn}$ denotes the (m, n)-th element. The notation $\|\cdot\|$ denote the 2-norm. $\mathcal{N}(0, \sigma^2)$ denotes a Gaussian distribution with a mean 0 and variance σ^2.

II. SYSTEM MODEL AND THE PD NORMAL VECTOR

A. SYSTEM MODEL

Consider an SM VLC system in Fig. 1 with N_t LEDs and a PD. In the system, an SM transmitter with a set of M-PAM symbols are employed, as shown in Fig. 1. The bit sequence with a length of $(R_1 + R_2)$ bits is divided into two parts, containing R_1 bits and R_2 bits, respectively [18]. The first part is used to select an active LED to convey modulated positive intensity information, while the other LEDs are inactive. In particular, the first $R_1 = \log_2(N_t)$ bits are mapped to a spatial constellation point drawn from the set with the cardinality N_t

$$\mathcal{S}_{\text{spatial}} = \{\mathbf{e}_1, \mathbf{e}_2, \ldots, \mathbf{e}_k, \ldots, \mathbf{e}_{N_t}\}, \tag{1}$$

where $\mathbf{e}_k$ is an $N_t \times 1$ vector with all elements zeros except the k-th element equal, which is equal to one. Then, the last $R_2 = \log_2(M)$ bits are mapped to a signal constellation point drawn from the set with the cardinality M

$$\mathcal{S}_{\text{constellation}} = \{s_1, s_2, \ldots, s_m, \ldots, s_M\}, \tag{2}$$

where $s_m \in \mathbb{R}^+$ is the m-th M-PAM level signal. If the k-th LED is activated and the m-th constellation point in M-PAM signal constellation is emitted, the one-dimensional transmitted SM signal vector $\mathbf{x}_i \in \mathcal{S}$ can be expressed as

$$\mathbf{x}_i = [0,\ldots,0,s_{km},0,\ldots,0]^T, \tag{3}$$

where set $\mathcal{S}$ with the cardinality N_tM is the combination between the spatial and constellation symbols and can be represented as

$$\mathcal{S} = \{\mathbf{e}_1 s_1, \mathbf{e}_1 s_2, \ldots, \mathbf{e}_1 s_M, \mathbf{e}_2 s_1, \ldots, \mathbf{e}_{N_t M}\}. \tag{4}$$

At the receiver, a PD receives the optical intensity signals and converts them into electrical signals. Assume perfect synchronization between transmitters and receiver [3], the received signal value at the PD can be written as

$$y = \mathbf{h}\mathbf{x}_i + w, \tag{5}$$

where y represents the received signal, and w is the noise. Moreover, w can be modeled as independent real-valued additive white Gaussian noise with zero mean and a variance of $\sigma_n^2 = \sigma_{\text{sh}}^2 + \sigma_{\text{th}}^2$, where σ_{th}^2 is the thermal noise variance [3]. The signal dependent shot noise with main source is the current of the PD can be mathematically described by a stationary Poisson random process and can be approximated by a Gaussian process with a variance of σ_{sh}^2 [19]. $\mathbf{h} = \begin{bmatrix} h_1 & h_2 & \dots h_j & \dots h_{N_t} \end{bmatrix}$ is the $(1 \times N_t)$-dimensional channel vector. On the other hand, the channel impulse response in indoor VLC systems generally consists of a LOS component and a non-LOS (NLOS) component due to reflections. In this paper, the LOS link is ensured to be always exist between any LED and the PD. Moreover, the LOS component is commonly assumed to be dominant and the NLOS components is much weaker that can be neglected [12]. Thus, as an initial exploration and for simplicity, we only consider LOS links between the transmitters and the receiver. The channel gain between the j-th LED and the PD can be modeled as

$$h_j = \frac{(\gamma + 1) A_p g}{2\pi d_j^2} \cos^{\gamma} \phi_j \cos \theta_j \Gamma\left(\theta_j, \theta_{\text{fov}}\right), \tag{6}$$

where ϕ_j is the emission angle from the j-th LED to the PD, θ_j is the angle of incidence at the PD due to the j-th LED, A_p is the PD area, and g is the gain of the optical concentrator. Moreover, θ_{fov} is the PD field of view semi-angle, d_j is the distance between the PD and j-th LED, and γ is the order of the generalized Lambertian radiation. The half-power semi-angle, $\Phi_{1/2}$, is related to γ as $\gamma = \frac{-\ln 2}{\ln(\cos \Phi_{1/2})}$. Moreover, the notation $\Gamma\left(\theta_j, \theta_{\text{fov}}\right)$ represents a rectangular function, given as

$$\Gamma\left(\theta_j, \theta_{\text{fov}}\right) = \begin{cases} 1 & \theta_j \leqslant \theta_{\text{fov}} \\ 0 & \theta_j > \theta_{\text{fov}}. \end{cases} \tag{7}$$

In particular, $\Gamma\left(\theta_j, \theta_{\text{fov}}\right)$ implies that the channel gain is zero if θ is larger than θ_{fov} equivalently the LED is outside the PD FOV. At the receiver, the maximum-likelihood detector is utilized to detect the received signal and can be expressed as

$$(\bar{\mathbf{e}}, \bar{s}) = \arg \min_{\mathbf{x}_i \in \mathcal{S}} \|y - \mathbf{h}\mathbf{x}_i\|^2. \tag{8}$$

B. THE NORMAL VECTOR OF THE PD

As illustrated in Fig. 2, ϕ_j, θ_j, and d_j denote the irradiance angle at the j-th LED with respect to the PD, the incident angle at the PD with respect to the j-th LED, and the distance between the j-th LED and the PD, respectively. Moreover, in (6), we can express

$$\cos \phi_j = \frac{\overrightarrow{T}_j \cdot \overrightarrow{V}_j}{\|\overrightarrow{T}_j\| \|\overrightarrow{V}_j\|}, \tag{9}$$

$$\cos \theta_j = \frac{-\overrightarrow{V}_j \cdot \overrightarrow{U}}{\|\overrightarrow{T}_j\| \|\overrightarrow{U}\|}, \tag{10}$$

where $\overrightarrow{T}_j$ represents the normal vector of the j-th LED with an irradiance direction, $\overrightarrow{V}_j$ denotes the vector from the j-th LED to the PD, and $\overrightarrow{U}$ is the normal vector of the PD in the incident direction. Moreover, equations (9) and (10) can be represented as

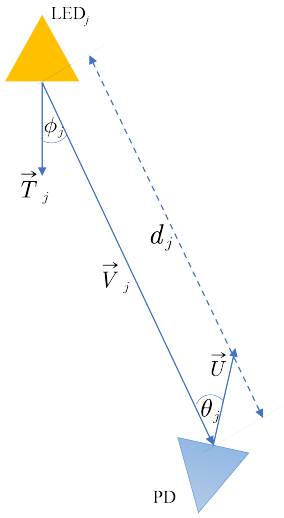

FIGURE 2. The geometry between an LED and a PD.

$$\cos \phi_j = \frac{\mathbf{t}_j^T \mathbf{v}_j}{\|\mathbf{t}_j\| \|\mathbf{v}_j\|}, \tag{11}$$

$$\cos \theta_j = \frac{-\mathbf{v}_j^T \mathbf{u}}{\|\mathbf{v}_j\| \|\mathbf{u}\|}, \tag{12}$$

where $\mathbf{t}_j$, $\mathbf{v}_j$, and $\mathbf{u}$ are the position vectors of $\overrightarrow{T}_j$, $\overrightarrow{V}_j$, and $\overrightarrow{U}$. Consequently, the channel coefficient in (6) can be rewritten as

$$h_j = \frac{(\gamma + 1) A_p g}{2\pi d_j^2} \left(\frac{\mathbf{t}_j^T \mathbf{v}_j}{\|\mathbf{t}_j\| \|\mathbf{v}_j\|} \right)^{\gamma} \frac{-\mathbf{v}_j^T \mathbf{u}}{\|\mathbf{v}_j\| \|\mathbf{u}\|} \Gamma\left(\theta_j, \theta_{\text{fov}}\right). \tag{13}$$

It can be seen that, theoretically, the vector $\mathbf{u}$ will directly affect the value of the channel coefficient h_j. Moreover, we can see from (6) that to successfully receive the transmit signal, the channel vector elements have to be highly distinguishable. The correlation between the wireless channel links may cause the received signal to be inseparable and hence should be avoided in a multiple LEDs system [16]. Therefore, in theory, to improve the performance of multiple transmitter elements in a VLC system, we can carefully alter the orientation of the receiver according to (13). In the next sections, we will explain novel methods to set the PD orientations so the orientation parameters can be utilized to aid the information transmission for a practical VLC system.

It is assumed that the location of LEDs and PD are fixed. Since the orientations of LEDs are fixed, the orientation of the PD can be specified by a normal vector with parameter $\overrightarrow{U}(\alpha, \beta)$ with $0 \leqslant \alpha \leqslant \pi$ and $0 \leqslant \beta \leqslant 2\pi$, as illustrated in Fig. 3, where β and α denote the elevation angle and the azimuth angle, respectively. In practice, the parameters β and α can be used to adjust the orientation of the PD to improve

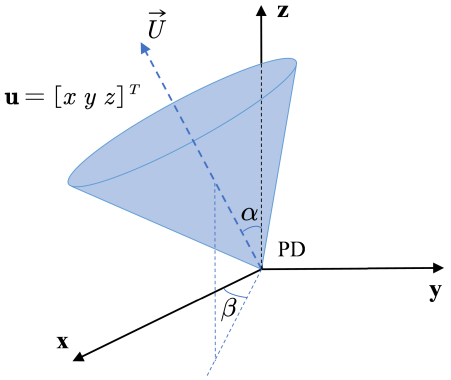

FIGURE 3. The coordinates of a PD's normal vector.

the system performance. Consequently, the normal vector can be expressed in a Cartesian coordinate as

$$\mathbf{u} \equiv \vec{U}\ (\alpha, \beta) \triangleq \begin{cases} x = \|\vec{U}\| \sin\alpha \cos\beta \\ y = \|\vec{U}\| \sin\alpha \sin\beta \\ z = \|\vec{U}\| \cos\alpha. \end{cases} \tag{14}$$

In our paper, we first optimize the normal vectors of the PD. Then, by transforming the optimized vector back to spherical coordinates, the resulting can be effectively utilized to orientate the PD and improve the system performance.

III. PROPOSED PD ORIENTATION FOR BER IMPROVEMENT

From (13), in the case of $0 \leqslant \theta_j \leqslant \theta_{\text{fov}}$, the channel coefficient h_j can be expressed as a function of the PD normal vector $\mathbf{u}$ as

$$h_j = q_j \left(\frac{-\mathbf{v}_j^T \mathbf{u}}{\|\mathbf{v}_j\| \|\mathbf{u}\|} \right), \tag{15}$$

with the constraint $q_j = \frac{(\gamma+1) A_p g}{2\pi d_j^2} \left(\frac{\mathbf{t}_j^T \mathbf{v}_j}{\|\mathbf{t}_j\| \|\mathbf{v}_j\|} \right)^{\gamma}$. Moreover, by defining $\hat{\mathbf{v}}_j^T = \frac{\mathbf{v}_j^T}{\|\mathbf{v}_j\|}$ and $\hat{\mathbf{u}} = \frac{\mathbf{u}}{\|\mathbf{u}\|}$, (15) can be rewritten as

$$h_j = q_j (-\hat{\mathbf{v}}_j)^T \hat{\mathbf{u}}. \tag{16}$$

Here, $\hat{\mathbf{u}}$ is the normalized vector, represented by $\hat{\mathbf{u}} = \left[\frac{x_{\text{PD}}}{\|\mathbf{u}\|} \ \frac{y_{\text{PD}}}{\|\mathbf{u}\|} \ \frac{z_{\text{PD}}}{\|\mathbf{u}\|} \right]^T$. Therefore, from (16), with the assumption that $0 \leqslant \theta_j \leqslant \theta_{\text{fov}}$, we derive that the channel vector can be represented as

$$\mathbf{h}^T = \mathbf{q} \circledast \mathbf{p}, \tag{17}$$

where $\circledast$ is element-wise product notation. In (17), $\mathbf{q}$ is the $N_t \times 1$ vector where each element q_j expresses the relation between the PD and the j-th LED, $\mathbf{p}$ is the $N_t \times 1$ vector, with each element is defined by $p_j = (-\hat{\mathbf{v}}_j)^T \hat{\mathbf{u}}$. Therefore, to better represent the received signal according to the orientation vector of the PD, we can rewrite the received signal in (5) as

$$y = \mathbf{x}_i^T\ (\mathbf{q} \circledast \mathbf{p}) + w. \tag{18}$$

Furthermore, from $p_j = (-\hat{\mathbf{v}}_j)^T \hat{\mathbf{u}}$, we have $\mathbf{p} = \hat{\mathbf{V}}\hat{\mathbf{u}}$, with $\hat{\mathbf{V}} = \begin{bmatrix} -\hat{\mathbf{v}}_1^T \\ \vdots \\ -\hat{\mathbf{v}}_{N_t}^T \end{bmatrix}$ is an $N_t \times 3$ matrix. After inserting $\mathbf{p}$ into (18), we can derive

$$\begin{aligned} y &= \mathbf{x}_i^T\ (\mathbf{q} \circledast \mathbf{p}) + w \\ &= \mathbf{x}_i^T \left[\mathbf{q} \circledast \left(\hat{\mathbf{V}}\hat{\mathbf{u}} \right) \right] + w \\ &= \mathbf{b}_i \hat{\mathbf{u}} + w, \end{aligned} \tag{19}$$

where the constraint vector $\mathbf{b}_i = \mathbf{x}_i^T \begin{bmatrix} q_1 \left(-\hat{\mathbf{v}}_1^T \right) \\ \vdots \\ q_{N_t} \left(-\hat{\mathbf{v}}_{N_t}^T \right) \end{bmatrix}$.

Generally, the average bit error probability can be approximated by considering the nearest neighbor approximation of the pairwise error probability [4]

$$P(\mathbf{h}) \leqslant \frac{1}{2^R \left(2^R - 1\right)} \sum_{\mathbf{x}_i} \sum_{\mathbf{x}_{i'} \neq \mathbf{x}_i} D_{\mathbf{x}_i \mathbf{x}_{i'}} Q \left(\sqrt{\frac{d_{\mathbf{x}_i \mathbf{x}_{i'}}(\mathbf{h})}{4N_0}} \right) \tag{20}$$

with $D_{\mathbf{x}_i \mathbf{x}_{i'}}$ is the Hamming distance between two bit assignments of symbol $\mathbf{x}_i$ and $\mathbf{x}_{i'}$, N_0 is the noise power. $Q(x) = \left(\frac{1}{\sqrt{2\pi}} \right) \int_x^{\infty} e^{\frac{-y^2}{2}} dy$ denotes the Gaussian tail probability. It is evident that the minimum ED between any two transmitted symbols $\mathbf{x}_i \neq \mathbf{x}_{i'} \in \mathcal{S}$, $d_{\mathbf{x}_i \mathbf{x}_{i'}}(\mathbf{h}) = [\mathbf{h}(\mathbf{x}_i - \mathbf{x}_{i'})]^2$ should be maximized to minimize the error rate. Therefore, to adjust the normal vectors of the PD for a BER performance improvement, the following ED-based decision metric is maximized in order to minimize the approximated error probability

$$\tilde{\mathbf{u}} = \arg\max_{\hat{\mathbf{u}}} \left[\min_{\mathbf{x}_i \neq \mathbf{x}_{i'} \in \mathcal{S}} (\mathbf{h}\mathbf{x}_i - \mathbf{h}\mathbf{x}_{i'})^2 \right]. \tag{21}$$

Based on the criterion of (21), the PD orientation vector optimization problem can be formulated as

$$\text{(P1):} \quad \max_{\hat{\mathbf{u}}, \theta_j} \min_{\mathbf{x}_i \neq \mathbf{x}_{i'} \in \mathcal{S}} [\mathbf{h}(\mathbf{x}_i - \mathbf{x}_{i'})]^2 \tag{22a}$$

$$s.t.\ 0 \leqslant \theta_j \leqslant \theta_{\text{fov}}, \tag{22b}$$

where the condition (22b) is used to ensure that the incident angle between the PD and any LED is smaller than the FOV of the PD and a LOS link exists between the PD and any LED. Moreover, from (19) and (21), the objective value can be represented as

$$\begin{aligned} d_{\mathbf{x}_i \mathbf{x}_{i'}}(\mathbf{u}) &= [\mathbf{h}(\mathbf{x}_i - \mathbf{x}_{i'})]^2 \\ &= \left[(\mathbf{b}_i - \mathbf{b}_{i'}) \hat{\mathbf{u}} \right]^2 \\ &= \hat{\mathbf{u}}^T \mathbf{\Delta}_{ii'} \hat{\mathbf{u}}, \end{aligned} \tag{23}$$

where $\mathbf{\Delta}_{ii'} = (\mathbf{b}_i - \mathbf{b}_{i'})^T (\mathbf{b}_i - \mathbf{b}_{i'})$ for any two $\mathbf{x}_i \neq \mathbf{x}_{i'} \in \mathcal{S}$.

Moreover, we can simplify the optimization problem by relaxing the condition that $\hat{\mathbf{u}} = \frac{\mathbf{u}}{\|\mathbf{u}\|}$ and set $\|\mathbf{u}\| = 1$ to make $\hat{\mathbf{u}} = \mathbf{u}$. This will lead to the constraint $\|\mathbf{u}\|^2 = 1$. Moreover, the condition (22b), with the help of (11) and $\|\mathbf{u}\| = 1$, can be expressed as $\cos\theta_{\text{fov}} \leqslant \hat{\mathbf{v}}_j^T \mathbf{u} \leqslant 1$. By applying these results

to the optimization problem (P1) and introducing an auxiliary variable ρ, we have the equivalent epigraph form [20] of (P2) as

$$\text{(P2):} \quad \max_{\mathbf{u}} \rho \tag{24a}$$

$$\text{s.t. } \mathbf{u}^T \mathbf{\Delta}_{ii'} \mathbf{u} \geqslant \rho \tag{24b}$$

$$\cos\theta_{\text{fov}} \leqslant \hat{\mathbf{V}}\mathbf{u} \leqslant 1 \tag{24c}$$

$$\|\mathbf{u}\|^2 = 1. \tag{24d}$$

Furthermore, the optimization problem (P2) is still non-convex due to the constraint (24b), (24d), and the problem (P2) is an NP-complete problem. On the other hand, the problem (P2) is a large-scale non-convex quadratically constrained quadratic program (QCQP) problem with the number of the quadratic constraints in (P2) is $2^{R-1}\left(2^R-1\right)+1$, and becomes very large for very large number of R. In small scale QCQP problems, semidefinite relaxation (SDR) [21] has been well known. SDR approximates this QCQP problem as a convex semidefinite programming problem via relaxation. In particularly, by setting $\mathbf{W} = \mathbf{u}\mathbf{u}^T$ and relaxing the problem through dropping the rank-one constraint of the matrix $\mathbf{W}$, a globally optimal solution can be obtained. However, with the increasing number of quadratic constraints, achieving rank-one or low rank solutions of $\mathbf{W}$ is very unlikely and making the SDR method ineffective. In the other hand, the constraint (24d) can be split into two constraints

$$\|\mathbf{u}\|^2 \leqslant 1, \tag{25a}$$

$$\|\mathbf{u}\|^2 \geqslant 1. \tag{25b}$$

To deal with the nonconvex constraints (24b) and (25b), by denoting $\mathbf{u}^{(k)}$ as the value of $\mathbf{u}$ at the k-th iteration and employing the linearization around $\mathbf{u}^{(k)}$, the left-hand side of the inequality in (24a) and (25b) can be approximated by

$$\mathbf{u}^T \mathbf{\Delta}_{ii'} \mathbf{u} \approx \mathbf{u}^T \mathbf{\Delta}_{ii'} \left(\mathbf{u}^{(k)}\right) + \left(\mathbf{u}^{(k)}\right)^T \mathbf{\Delta}_{ii'} \mathbf{u} - \left(\mathbf{u}^{(k)}\right)^T \mathbf{\Delta}_{ii'} \mathbf{u}^{(k)}, \tag{26}$$

$$\|\mathbf{u}\|^2 \approx \mathbf{u}^T \left(\mathbf{u}^{(k)}\right) + \left(\mathbf{u}^{(k)}\right)^T \mathbf{u} - \left(\mathbf{u}^{(k)}\right)^T \mathbf{u}^{(k)}. \tag{27}$$

Finally, the optimization problem (P2) can be reformed as

$$\text{(P3):} \quad \max_{\mathbf{u}} \rho \tag{28a}$$

$$\text{s.t. } \mathbf{u}^T \mathbf{\Delta}_{ii'} \left(\mathbf{u}^{(k)}\right) + \left(\mathbf{u}^{(k)}\right)^T \mathbf{\Delta}_{ii'} \mathbf{u} - \left(\mathbf{u}^{(k)}\right)^T \mathbf{\Delta}_{ii'} \mathbf{u}^{(k)} \geqslant \rho \tag{28b}$$

$$\cos\theta_{\text{fov}} \leqslant \hat{\mathbf{V}}\mathbf{u} \leqslant 1 \tag{28c}$$

$$\mathbf{u}^T\mathbf{u} \leqslant 1 \tag{28d}$$

$$\mathbf{u}^T \left(\mathbf{u}^{(k)}\right) + \left(\mathbf{u}^{(k)}\right)^T \mathbf{u} - \left(\mathbf{u}^{(k)}\right)^T \mathbf{u}^{(k)} \geqslant \mathbf{1}. \tag{28e}$$

It is observed that (P3) is a convex optimization problem that can be conveniently solved by the CVX optimization package [22] with the primal-dual interior point method. In particular, by initializing a point $\mathbf{u}^{(0)}$ and iteratively solving (P3) until convergence, we can obtain a sequence of solutions $\mathbf{u}^{(k)}$ and the last one can be used as an approximated solution to (P1). This method is able to achieve a favorable error performance in the simulations with a wise choice of the initial solution. To obtain different initial solutions for the optimization solver, a method is required to generate a number of initial normal vectors. Since with the PD, the set of all normal vectors form a sphere with the center at the location of the PD and a radius equal to one. More specifically, we divide the unit sphere to $2N$ points with N equaling the number of initial points required for the solver. For $1 \leqslant l \leqslant N$, the initial normal vector $\mathbf{u}_l$ can be calculated from (14) with α_l and β_l defined as in [14], [23]

$$\alpha_l = \arccos\left(t_l\right), \tag{29}$$

and with

$$\beta_l = \left(\beta_{l-1} + \frac{3.6}{\sqrt{2N}} \frac{1}{\sqrt{1-t_l^2}}\right) \mod (2\pi), \ 2 \leqslant l \leqslant N, \tag{30}$$

where $\beta_1 = 0$ and $t_l = 1 - \frac{2(l-1)}{2N-1}$. The $\mod(2\pi)$ factor in (30) ensures that the angle is inside the range of $[0,2\pi]$. Then, we take a number of initial solutions $\overrightarrow{U_l}(\alpha, \beta)$ that satisfy the FOV condition, and the solver will iteratively run and find the optimal normal vector for the problem (P3) that derives the largest value of ρ_l. In our simulation, it is shown that an acceptable number of initial points can provide an optimal solution and this method offers a significantly improved BER performance. Moreover, the detail steps to find the PD normal vector are given in Algorithm 1 where N, $\mathbf{\Theta}$, $\xi_{\text{convergence}}$, and $\mathbf{u}^\dagger$ are the number of initial realization of $\mathbf{u}$, the set of initial realization of $\mathbf{u}$, the convergence threshold, and the solution of solving (P3) respectively.

IV. PD ORIENTATION FOR CHANNEL CAPACITY IMPROVEMENT

In this section, by altering the PD orientation, we seek to improve the achievable performance of the SM VLC scheme in terms of the instantaneous channel capacity, in a manner similar to the approaches used in previous studies [24]. In the literature, near-capacity performance can be attained in practice scenarios with the aid of powerful channel-coding schemes, such as turbo and low-density parity-check codes [19]. Specifically, the instantaneous unconstrained channel capacity of the SM VLC system can be bounded below by

$$C_{SM} \geqslant \frac{1}{N_t} \sum_{j=1}^{N_t} \log\left(1 + \frac{P}{\sigma_n^2 B_{\text{W}}} h_j^2\right) = \frac{1}{N_t} \sum_{j=1}^{N_t} \log\left(1 + \eta h_j^2\right), \tag{31}$$

Algorithm 1 Iterative Algorithm for Solving (P3)

Input: initial vectors $\mathbf{u}_1, \ldots, \mathbf{u}_{N_{\text{ite}}}$.
Output: normal vector $\mathbf{u}_{\max}$

```
innitialization Θ ← ∅, ρ_max = 0
for l = 1 ... N_ite do
    generate U_l (α_l, β_l) from (29), (30)
    obtain u_l equivalent to U_l (α_l, β_l)
    if _fov ⩽ V̂ u_l ⩽ 1 then
        set Θ ← Θ + {u_l}
    end if
end for
for u_l ∈ Θ do
    set k = 1
    set ρ^(0) = 0, u^(0) = u_l
    while ρ^(k) − ρ^(k−1) ⩾ ξ_convergence do
        normalize u^(k−1)
        solve (P3) with the input as u^(k−1) to get the solution u†
        update u^(k) = u†
        set k = k + 1
    end while
    if ρ^(k−1) ⩾ ρ_max then
        set ρ_max = ρ^(k−1)
        set u_max = u^(k−1)
    end if
end for
return the normal vector u_max
```

where $\eta = \frac{P}{\sigma_n^2 B_{\text{W}}}$ is the average signal-to-noise ratio (SNR) at the receive PD. P is the transmit power of each LED and B_{W} is the bandwidth. Moreover, for the j-th LED, the channel coefficient h_j that represents the column channel corresponding to the j-th column of the channel vector $\mathbf{h}$ can be expressed as

$$h_j = p_j q_j. \tag{32}$$

We mentioned again that for the j-th LED, we have $p_j = -\hat{\mathbf{v}}_j^T \hat{\mathbf{u}}$ and $q_j = \frac{(\gamma+1)A_p}{2\pi d_j^2} \cos^\gamma \alpha_j$ for the PD. Therefore, for the j-th LED, the corresponding channel coefficient is

$$h_j = q_j(-\hat{\mathbf{v}}_j)^T \hat{\mathbf{u}} = \mathbf{t}_j^T \hat{\mathbf{u}}, \tag{33}$$

where $\mathbf{t}_j^T = -q_j \hat{\mathbf{v}}_j^T$ for j-th LED. Consequently, by utilizing the result in (33), the channel capacity can be lower bounded by

$$\begin{aligned} C_{SM} &\geqslant \frac{1}{N_t} \sum_{j=1}^{N_t} \log\left(1 + \eta \hat{\mathbf{u}}^T \mathbf{t}_j \mathbf{t}_j^T \hat{\mathbf{u}}\right) \\ &= \frac{1}{N_t} \sum_{j=1}^{N_t} \log\left[1 + \text{tr}\left(\mathbf{G}_j \hat{\mathbf{W}}\right)\right], \end{aligned} \tag{34}$$

where $\mathbf{G}_j = \eta \mathbf{t}_j \mathbf{t}_j^T = \eta \left(q_j\right)^2 \hat{\mathbf{v}}_j \hat{\mathbf{v}}_j^T$ and $\hat{\mathbf{W}} = \hat{\mathbf{u}}\hat{\mathbf{u}}^T$.

Similar to the optimization problem (P3), we maximize the lower bound of the channel capacity by forming the following optimization problem

$$\text{(P4):} \quad \max_{\hat{\mathbf{W}}, \theta_j} \frac{1}{N_t} \sum_{j=1}^{N_t} \log\left[1 + \text{tr}\left(\mathbf{G}_j \hat{\mathbf{W}}\right)\right] \tag{35a}$$

$$s.t.\ 0 \leqslant \theta_j \leqslant \theta_{\text{fov}} \tag{35b}$$

$$\hat{\mathbf{W}} \succcurlyeq 0 \tag{35c}$$

$$\text{rank}\left(\hat{\mathbf{W}}\right) = 1. \tag{35d}$$

Again, we aim to relax the optimization problem (P4) by setting $\|\mathbf{u}\| = 1$ to make $\hat{\mathbf{u}} = \mathbf{u}$ and consequently, $\hat{\mathbf{W}} = \hat{\mathbf{u}}\hat{\mathbf{u}}^T = \mathbf{u}\mathbf{u}^T = \mathbf{W}$. This will lead to the additional constraint $\text{tr}(\mathbf{W}) = 1$. On the other hand, from constraint (35b), we then have

$$\cos\theta_{\text{fov}} \leqslant -\hat{\mathbf{v}}_j^T \mathbf{u} \leqslant 1. \tag{36}$$

If we assume that $0 \leqslant \theta_{\text{fov}} \leqslant \pi$, the constraints in (34) can be equivalently represented as

$$\cos^2\theta_{\text{fov}} \leqslant \mathbf{u}^T \hat{\mathbf{v}}_j \hat{\mathbf{v}}_j^T \mathbf{u} \leqslant 1, \tag{37}$$

or

$$\cos^2\theta_{\text{fov}} \leqslant \text{tr}\left(\hat{\mathbf{V}}_j \mathbf{W}\right) \leqslant 1, \tag{38}$$

where $\hat{\mathbf{V}}_j = \hat{\mathbf{v}}_j \hat{\mathbf{v}}_j^T$.

Finally, the optimization problem (P4) can be reformed as

$$\text{(P5):} \quad \max_{\mathbf{W}, \theta_j} \frac{1}{N_t} \sum_{j=1}^{N_t} \log\left[1 + \text{tr}\left(\mathbf{G}_j \mathbf{W}\right)\right] \tag{39a}$$

$$s.t.\ \cos^2\theta_{\text{fov}} \leqslant \text{tr}\left(\hat{\mathbf{V}}_j \mathbf{W}\right) \leqslant 1 \tag{39b}$$

$$\text{tr}(\mathbf{W}) = 1 \tag{39c}$$

$$\mathbf{W} \succcurlyeq 0 \tag{39d}$$

$$\text{rank}(\mathbf{W}) = 1. \tag{39e}$$

The last obstacle in solving (P5) is to deal with the non-convex rank-one constraint $\text{rank}(\mathbf{W}) = 1$. By relaxing the rank constraint of $\mathbf{W}$, the problem (P5) can be approximated by the following SDR problem

$$\text{(P6):} \quad \max_{\mathbf{W}, \theta_j} \frac{1}{N_t} \sum_{j=1}^{N_t} \log\left[1 + \text{tr}\left(\mathbf{G}_j \mathbf{W}\right)\right] \tag{40a}$$

$$s.t.\ \text{tr}\left(\hat{\mathbf{V}}_j \mathbf{W}\right) \geqslant \cos^2\theta_{\text{fov}} \tag{40b}$$

$$\text{tr}\left(\hat{\mathbf{V}}_j \mathbf{W}\right) \leqslant 1 \tag{40c}$$

$$\text{tr}(\mathbf{W}) = 1 \tag{40d}$$

$$\mathbf{W} \succcurlyeq 0. \tag{40e}$$

Problem (P6) is a convex optimization problem, which can be solved optimally and efficiently by using available software packages, such as CVX [22]. However, due to the relaxation, the SDR solution to problem (P6) may have rank greater than one. For that case, various kinds of approximation such as randomization are required to find the suboptimal normal vectors [21]. Even though the relaxation was

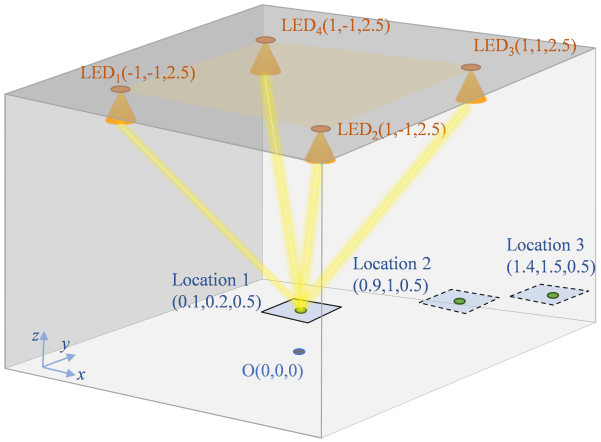

FIGURE 4. The simulation scenarios for 4-LED cases.

included, the optimal solution of (P6) obtained by using the SDR technique is found to be rank-one. This means that the optimal solution is exactly the same as that of (P5). The detailed proof is given in the Appendix. Moreover, through many simulation scenarios, the results always yield a rank one solution and therefore, we can obtain a global solution of the PD normal vector. On the other hand, assume that $\mathbf{u}^*$ is the vector that satisfies $\mathbf{u}^*(\mathbf{u}^*)^T = \mathbf{W}$. In the last step, to obtain a valid normal vector of the PD, due to the transformation from (36) to (37), only one of two conditions, $\cos\theta_{\text{fov}} \leqslant -\hat{\mathbf{v}}_j^T\mathbf{u}^* \leqslant 1$ or $\cos\theta_{\text{fov}} \leqslant -\hat{\mathbf{v}}_j^T(-\mathbf{u}^*) \leqslant 1$, is always satisfies and $\mathbf{u}^*$ or $-\mathbf{u}^*$ is selected as the optimal normal vector for the PD if the corresponding condition is satisfied.

V. NUMERICAL RESULTS

In this section, we show BER performance and the channel capacity of the proposed PD orientation schemes compared with the conventional cases. For the simulation, a VLC system with multiple LEDs and a PD is considered in a $4 \times 4 \times 2.5$m room, as illustrated in Fig. 4. We give the performance results with two scenarios. In the first case, a VLC system with four LEDs are fixed in a square shape with the location of LEDs at (1,1,2.5)m, (1,−1,2.5)m, (−1,1,2.5)m, and (−1,−1,2.5)m. The receiver is equipped with a PD and can be placed at three different locations in the room, and the coordinates of the receivers are (0.1,0.2,0.5)m, (0.9,1,0.5)m, and (1.4,1.5,0.5)m. Similarly, eight LEDs are used in the second SM VLC case. The LEDs are fixed at (1,1,2.5)m, (1,−1,2.5)m, (−1,1,2.5)m, (−1,−1,2.5)m, (1,0,2.5)m, (0,1,2.5)m, (−1,0,2.5)m, and (0,−1,2.5)m. The receiver equipped with one PD is also placed in three different locations, as in the previous scenario. The average transmission of electrical power between the LEDs is identical to the 4-LED case. Likewise, the average transmission of electrical power between the 8-LED cases are the same. In our simulation, the bit rate is set to $R = 4$ bps/Hz and $R = 6$ bps/Hz, respectively. Conventionally, following the assumption in various studies, the no orientation case is the

TABLE 1. Simulation parameters.

Parameters	Value
Room size	$4 \times 4 \times 2.5\text{m}^3$
Type of transmit and receive arrays	Square array
Number of transmit LEDs	4 or 8
Number of receive photodetectors	1
Channels	LOS
Bandwidth	40 MHz
The optical concentrator gain	1
Height of transmitter	0.5 m
Transmitter semiangle	60 deg
Field-of-view of photodetectors	60 deg
Photodetector area A	$1 \times 10^{-4}\text{m}^2$
Photodetector responsivity	1 A/W
Noise current density of transimpedance amplifier	2.5 pA/$\sqrt{\text{HZ}}$

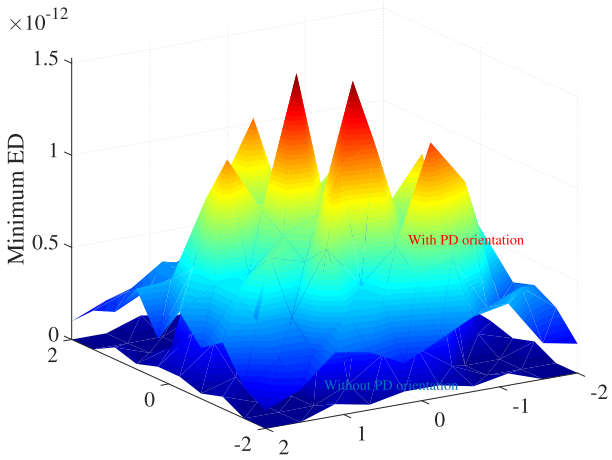

FIGURE 5. Minimum ED comparison in the 4-LED scenario with $R = 4$ bps/Hz.

case in which the normal vector of the PD is set to be the vector $[0\ 0\ 1]^T$. More detailed simulation parameters are provided in Table 1.

A. BER PERFORMANCE

To demonstrate the overall performance improvement of the proposed scheme in comparison with the conventional one, in Fig. 5, the minimum EDs of both schemes are shown for the case of 4-LED and $R = 4$ bps/Hz. The minimum ED values are shown for 100 locations uniformly distributed around the room with the same system parameter as defined in Table 1. Since the Algorithm 1 can only find the local solution corresponding to each initial point, the resulted minimum ED values appear to be largely vary. Moreover, since in the positions near center of the room, the PD is able to receive stronger signal from LEDs. This lead to larger minimum ED value and hence better BER performance in comparison with positions far from the center. It worth mentioning that in the corner locations, where without the orientation of PD, some LEDs are outside of the PD's FOV. This lead to the zero values of the minimum EDs and it is impossible for the receiver to properly function. In the other hand, with the aid of efficiently orientate the PD, the proposed scheme can

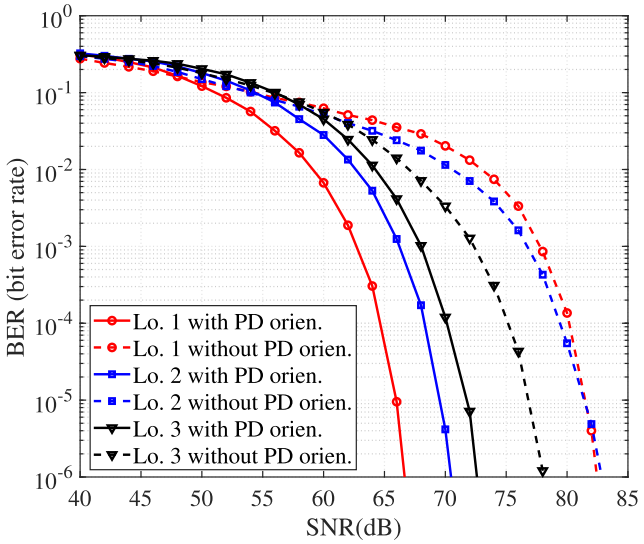

FIGURE 6. Performance comparison in the 4-LED scenario with $R = 4$ bps/Hz.

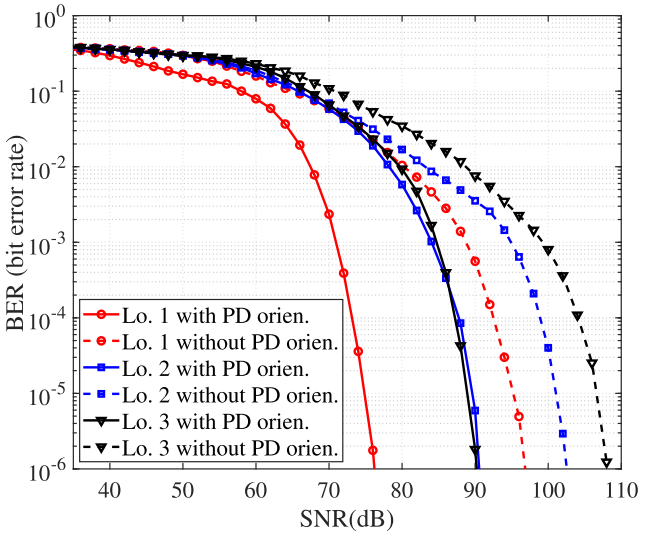

FIGURE 7. Performance comparison of the 4-LED scenario with $R = 6$ bps/Hz.

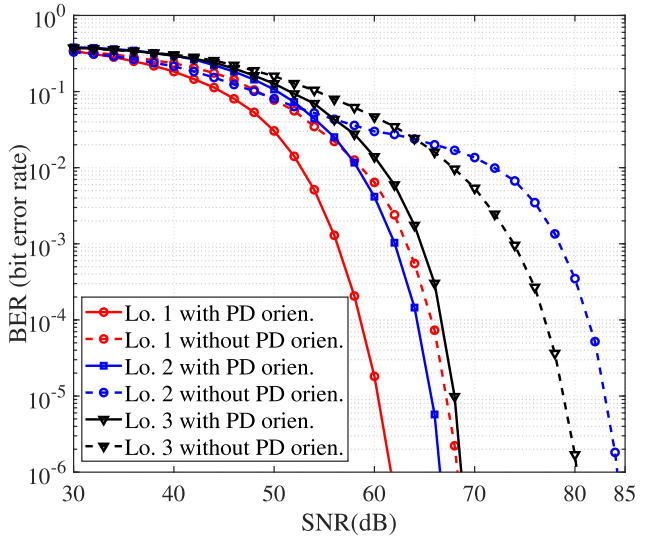

FIGURE 8. Performance comparison in the 8-LED scenario with $R = 4$ bps/Hz.

remarkably increase the minimum ED at various locations around the room.

To analyze the performance gain in specific SNR level, in Fig. 6 the BER performance comparison for the 4 bps/Hz 4×1 system with various locations of the PD is presented. With the proposed PD orientation, the nearer the location of the PD to the center of the room, the lower the BER performance of the SM VLC system. Moreover, the proposed method that changes the PD orientation can increase the SNR by as much as 15 dB in comparison with the no orientation case. In the locations of Location 1 and Location 2, due to the correlation between the channel coefficients caused by equivalent distances between the PD and some of the LEDs, the performance is greatly degraded. Therefore, by successfully decorrelating the channel coefficients by changing the normal vector of the PD, the proposed method can significantly improve the BER.

Similarly, in Fig. 7, the performance is analyzed for the case of $R = 6$ bps/Hz. The SNR gaps still maintain at least a 13 dB to 20 dB difference between the proposed method and the original ones. It is worth mentioning that in some special locations such as the center of the room, where the two distances between the PD and the two LEDs are relatively similar, without PD orientation, the receiver cannot distinguish between the two LEDs. Therefore, this issue causes the error floor phenomenon in the BER performance of the system. By changing the PD orientation, the magnitudes of the links between the PD and the LEDs are sufficiently different, which helps to alleviate the error floor problem and consequently improve the BER performance.

To demonstrate the effectiveness of the proposed method in the scenarios for larger number of LEDs, we show the BER performance of an 8×1 SM VLC system, with the data rate of $R = 4$ bps/Hz and $R = 6$ bps/Hz in Fig. 8 and Fig. 9, respectively. It can be noticed that with similar values of R, the system with more LEDs can exploit the availability of a higher spatial resource to transmit a larger number of bits. Therefore, with the same bit rate, the 8×1 system can achieve a lower BER in comparison with the 4×1 system. On the other hand, as in 4×1 case, the proposed method still maintains good performance improvement. Since the proposed method is only able to find the local solution of the optimization problem (P1), the optimality of the result of the PD normal vector is relatively acceptable in the sense of performance gain. The higher the number of initial solutions and iterations, the higher the chance of finding the global solution of the problem.

1) EXTENSION TO THE CONSIDERATION OF SIGNAL DEPENDENT NOISE

Moreover, in the practical VLC systems, due to the random nature of photon emission in the LED and the significant background light noise, shot noise can be depend on the

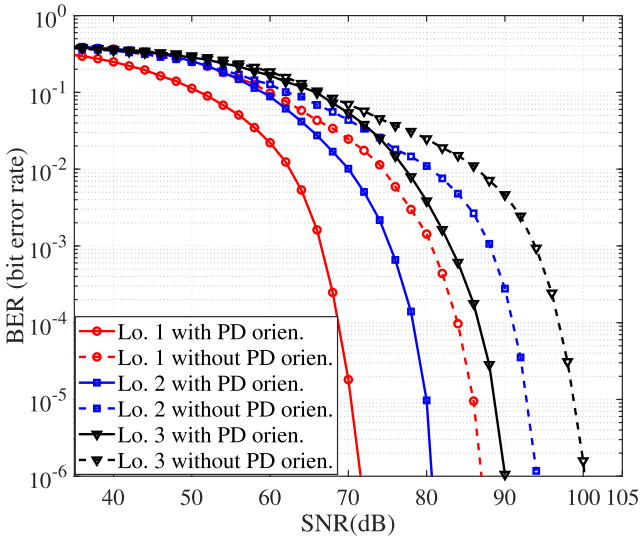

FIGURE 9. Performance comparison in in the 8-LED scenario with $R = 6$ bps/Hz.

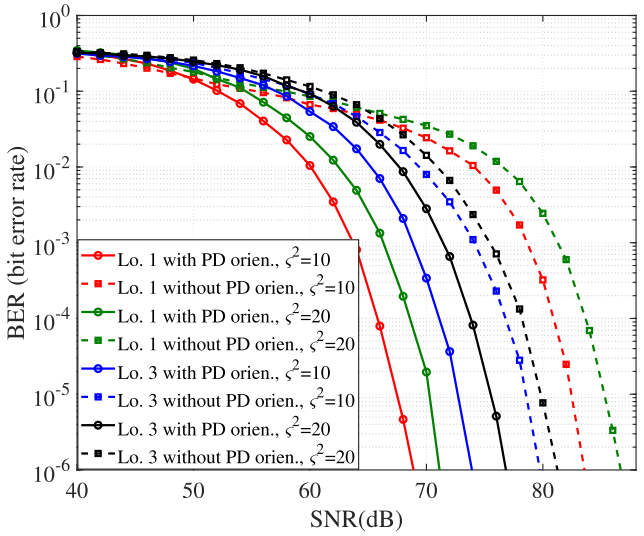

FIGURE 10. Performance comparison of the 4-LED scenario in Location 1 and Location 3 with $R = 4$ bps/Hz and $\varsigma^2 = 10, 20$.

transmitted signal [10]. In the followings, we show the analysis and performance of proposed scheme when the signal dependent noise is taken into account. As mentioned previously, the total noise can be expressed as $w = w_{\text{th}} + w_{\text{sh}}$, where the thermal noise is $w_{\text{th}} = \mathcal{N}\left(0, \sigma_{\text{th}}^2\right)$. More specifically, the shot noise variance that contributes to the signal dependent noise part when $\mathbf{x}_i$ is transmitted is $\sigma_{\text{sh}}^2 = \mathbf{hx}_i \varsigma^2 \sigma_{\text{th}}^2$, where ς^2 is the scaling factor of shot noise variance. This component causes the noise that depends on the intensity of the transmitted signal and can be modeled as $w_{\text{sh}} = \mathcal{N}\left(0, \mathbf{hx}_i \varsigma^2 \sigma_{\text{th}}^2\right)$. Consequently, the pairwise error probability with the contribution of signal dependent noise [25], [26] can be expressed as

$$P\left(\mathbf{x}_i \to \mathbf{x}_{i'}\right) = P\left(\frac{\frac{1}{2\pi\sigma_{\text{th}}\sqrt{\mathbf{hx}_{i'}\varsigma^2+1}} \exp\left\{\frac{-(y-\mathbf{hx}_{i'})^2}{2\sigma_{\text{th}}^2(\mathbf{hx}_{i'}\varsigma^2+1)}\right\}}{\frac{1}{2\pi\sigma_{\text{th}}\sqrt{\mathbf{hx}_i\varsigma^2+1}} \exp\left\{\frac{-(y-\mathbf{hx}_i)^2}{2\sigma_{\text{th}}^2(\mathbf{hx}_i\varsigma^2+1)}\right\}} > 1\right). \quad (41)$$

Clearly, the upper bound of the average error probability [4] is no longer dominant by the general minimum ED in (23). To alleviate the abnormal destructive impact of the signal dependent noise on the received signal, a new modified ED metric [25], [26], namely rotated-ED between any two signals, can be expressed as

$$d_{\mathbf{x}_i\mathbf{x}_{i'}}^{\text{sh}} = \left(\mathbf{hx}_i - \mathbf{hx}_{i'}\right)^T G_i^{-\frac{1}{2}} G_{i'}^{-\frac{1}{2}} \left(\mathbf{hx}_i - \mathbf{hx}_{i'}\right), \quad (42)$$

where $G_i = \mathbf{hx}_i\varsigma^2 + 1 = \mathbf{b}_i\hat{\mathbf{u}}\varsigma^2 + 1$ and $G_{i'} = \mathbf{hx}_{i'}\varsigma^2 + 1 = \mathbf{b}_{i'}\hat{\mathbf{u}}\varsigma^2 + 1$. Therefore, with $\|\mathbf{u}\| = 1$, the objective function instead of (23) becomes

$$d_{\mathbf{x}_i\mathbf{x}_{i'}}^{\text{sh}}(\mathbf{u}) = \frac{\mathbf{u}^T \boldsymbol{\Delta}_{ii'} \mathbf{u}}{\sqrt{\left(\mathbf{b}_i\mathbf{u}\varsigma^2 + 1\right)\left(\mathbf{b}_{i'}\mathbf{u}\varsigma^2 + 1\right)}}. \quad (43)$$

Consequently, through similar transformations as with (P3), the optimization problem with the new objective function can be reformed as

$$\begin{aligned}
(\text{P7}): \quad & \max_{\mathbf{u}} \ \rho && (44a)\\
& s.t.\ d_{\mathbf{x}_i\mathbf{x}_{i'}}^{\text{sh}}\left(\mathbf{u}^{(k)}\right) + \nabla d_{\mathbf{x}_i\mathbf{x}_{i'}}^{\text{sh}}\left(\mathbf{u}^{(k)}\right)\left(\mathbf{u} - \mathbf{u}^{(k)}\right) \geqslant \rho && (44b)\\
& \cos\theta_{\text{fov}} \leqslant \hat{\mathbf{V}}\mathbf{u} \leqslant 1 && (44c)\\
& \mathbf{u}^T\mathbf{u} \leqslant 1 && (44d)\\
& \mathbf{u}^T\left(\mathbf{u}^{(k)}\right) + \left(\mathbf{u}^{(k)}\right)^T\mathbf{u} - \left(\mathbf{u}^{(k)}\right)^T\mathbf{u}^{(k)} \geqslant \mathbf{1}. && (44e)
\end{aligned}$$

The constraint (44b) is the approximation of the non-convex distance constraint (43) using the first order Taylor series at $\mathbf{u}^{(k)}$, where $\nabla d_{\mathbf{x}_i\mathbf{x}_{i'}}^{\text{sh}}\left(\mathbf{u}^{(k)}\right)$ denotes the gradient for $d_{\mathbf{x}_i\mathbf{x}_{i'}}^{\text{sh}}(\mathbf{u})$, which can be referred to [26] (eq. (22))

$$\begin{aligned}
&\nabla d_{\mathbf{x}_i\mathbf{x}_{i'}}^{\text{sh}}\left(\mathbf{u}^{(k)}\right)\\
&= 2\left(\mathbf{u}^{(k)}\right)^T \boldsymbol{\Delta}_{ii'} G_i^{-\frac{1}{2}} G_{i'}^{-\frac{1}{2}}\\
&\quad - \frac{\varsigma^2}{2}\left(\mathbf{u}^{(k)}\right)^T \boldsymbol{\Delta}_{ii'}\mathbf{u}^{(k)}\left[G_i^{-\frac{1}{2}} G_{i'}^{-\frac{3}{2}}\mathbf{b}_{i'} + G_i^{-\frac{3}{2}} G_{i'}^{-\frac{1}{2}}\mathbf{b}_i\right].
\end{aligned} \quad (45)$$

The optimization (P7) can be conveniently solved by the iterative Algorithm 1 by the CVX optimization package [22].

Intuitively, under the impact of the signal dependent noise, performance of the ML detector that only optimally work under the signal independent noise assumption is indisputably degraded, for both proposed and conventional schemes. This is clearly illustrated in Fig. 10, where the performance comparison between proposed PD orientation and conventional one for a 4-LED scenario is shown in Location 1 and Location 3, with the transmission rate of $R = 4$ bps/Hz. For the shot noise component, we set $\varsigma^2 = 10, 20$. It is worth mentioning that in the previous case that does not consider

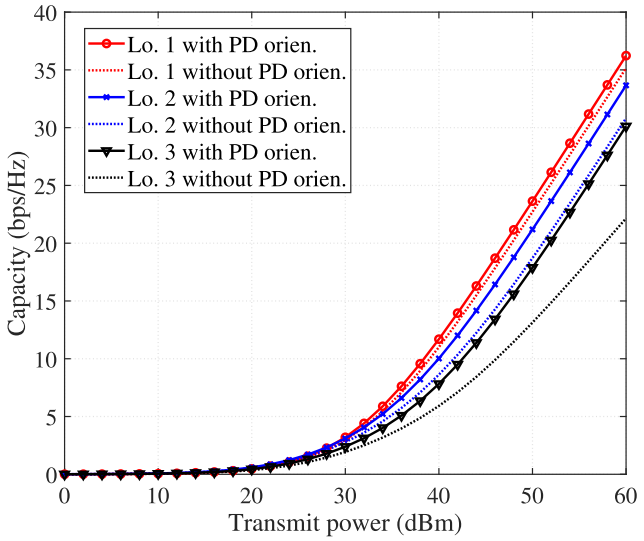

FIGURE 11. The capacity comparison in the 4-LED scenario.

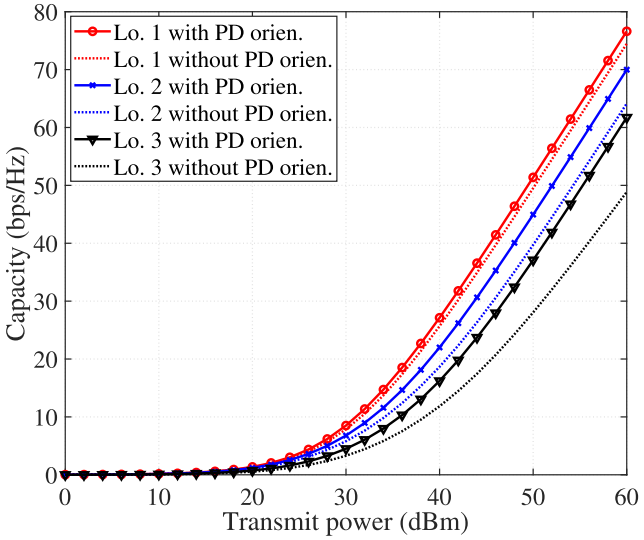

FIGURE 12. The capacity comparison in the 8-LED scenario.

the signal dependent noise, $\varsigma^2 = 0$. As in Fig. 10, BER performances of both schemes similarly degrade under the signal dependent noise impact. However, as expected, the proposed PD orientation still maintains significant SNR gaps in comparison with the conventional ones. Moreover, the higher the value of ς^2, the more severe impact of the signal dependent noise on both proposed and conventional schemes. Therefore, it can be concluded, the proposed scheme still provide greater BER improvement in comparison with the no orientation case, though performance degradation is expected.

B. CHANNEL CAPACITY PERFORMANCE

In Fig. 11 and Fig. 12, the unbounded channel capacity of the system for both the 4 and 8 LED scenarios are shown in term of bps/Hz. It is observed that with the case of location 1, since the LOS paths from the PD to all LEDs are relatively strong without altering the PD normal vector, the capacity

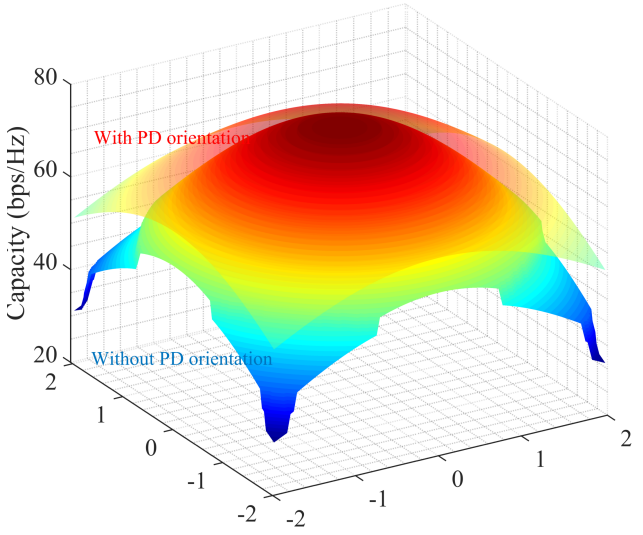

FIGURE 13. The capacity comparison for the 8-LED scenario with various PD locations in the room.

gain in this case is relatively small. However, as the PD becomes located further from the center, the proposed method shows a better capacity enhancement. As seen in Fig. 11, with the positioning of Location 3, at the level of transmit power of 60 dBm, the gain is around 8 bps/Hz. The capacity gap in for the 8-LED case increases to 15 bps/Hz and continues to increase commensurately with the transmit power.

To show the impact of the PD location on the channel capacity of the SM VLC system, in Fig. 13, the performance of the proposed method is compared with the conventional one. The channel capacity results are shown for various locations of the receiver inside the room. Overall, the capacity of the proposed method shows better results, especially at the corner and off-center locations of the room.

1) EXTENSION TO THE CONSIDERATION OF SIGNAL DEPENDENT NOISE

In this part, we again investigate the channel capacity improvement of proposed scheme under the influence of signal dependent noise. We define the channel capacity of spatial modulation system with the noise variance $\sigma_{\mathrm{n}}^2 = \sigma_{\mathrm{th}}^2\left(1 + \mathbf{h}\mathbf{x}_i\varsigma^2\right)$ by

$$C_{SM} \geqslant \frac{1}{2^R}\sum_{i=1}^{2^R}\log\left(1 + \eta\frac{(\mathbf{h}\mathbf{e}_i)^2}{\left(\mathbf{h}\mathbf{x}_i\varsigma^2 + 1\right)}\right), \tag{46}$$

where $\mathbf{e}_i$ is the vector obtained by replacing the only non-zero element of $\mathbf{x}_i$ by 1. Moreover, from (19) we have

$$\frac{(\mathbf{h}\mathbf{e}_i)^2}{\mathbf{h}\mathbf{x}_i\varsigma^2 + 1} = \frac{\hat{\mathbf{u}}^T\Lambda_i\hat{\mathbf{u}}}{\varsigma^2\mathbf{b}_i\hat{\mathbf{u}} + 1}, \tag{47}$$

where $\Lambda_i = \hat{\mathbf{b}}_i^T\hat{\mathbf{b}}_i$ and $\hat{\mathbf{b}}_i = \mathbf{e}_i^T\begin{bmatrix} q_1\left(-\hat{\mathbf{v}}_1^T\right) \\ \vdots \\ q_{N_{\mathrm{t}}}\left(-\hat{\mathbf{v}}_{N_{\mathrm{t}}}^T\right)\end{bmatrix}$. Consequently, with the auxiliary variable β_i and constraint

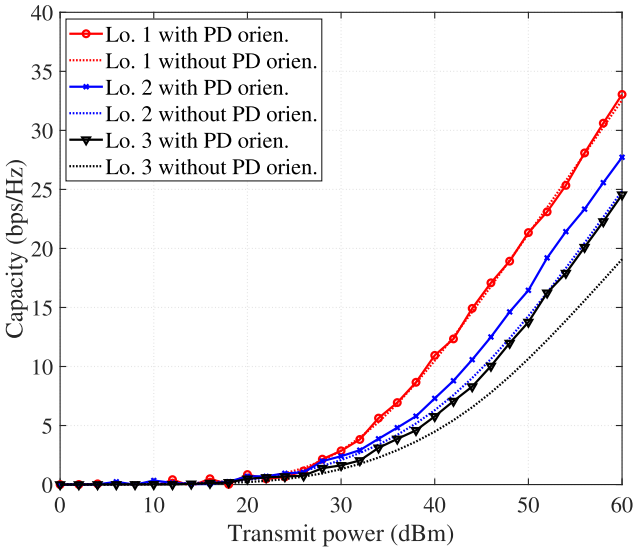

FIGURE 14. The capacity comparison for the 4-LED scenario with various PD locations in the room with $\varsigma^2 = 20$.

$\|\mathbf{u}\|^2 = 1$, we have the following channel capacity maximization optimization problem as

$$\text{(P8):} \quad \max_{\mathbf{u},\beta_i} \frac{1}{2^R}\sum_{i=1}^{2^R}\log\left(1+\eta\beta_i\right) \tag{48a}$$

$$s.t.\ \frac{\mathbf{u}^T\Lambda_i\mathbf{u}}{\varsigma^2\mathbf{b}_i\mathbf{u}+1} \geqslant \beta_i \tag{48b}$$

$$\cos\theta_{\text{fov}} \leqslant \hat{\mathbf{V}}\mathbf{u} \leqslant 1 \tag{48c}$$

$$\|\mathbf{u}\|^2 = 1. \tag{48d}$$

Again, the optimization problem (P8) is non-convex due to the constrain (48b). However, the left side of (48b), $f(\mathbf{u}) = \frac{\mathbf{u}^T\Lambda_i\mathbf{u}}{\varsigma^2\mathbf{b}_i\mathbf{u}+1}$ is the general quadratic-over-linear function [20]. By employing the first order Taylor expansion and with similar steps as in (P3), the problem (P8) can be approximated as

$$\text{(P9):} \quad \max_{\mathbf{u},\beta_i} \frac{1}{2^R}\sum_{i=1}^{2^R}\log\left(1+\eta\beta_i\right) \tag{49a}$$

$$\text{s.t.}\ f\left(\mathbf{u}^{(k)}\right) + \nabla f\left(\mathbf{u}^{(k)}\right)\left(\mathbf{u}-\mathbf{u}^{(k)}\right) \geqslant \beta_i \tag{49b}$$

$$\cos\theta_{\text{fov}} \leqslant \hat{\mathbf{V}}\mathbf{u} \leqslant 1 \tag{49c}$$

$$\mathbf{u}^T\mathbf{u} \leqslant 1 \tag{49d}$$

$$\mathbf{u}^T\left(\mathbf{u}^{(k)}\right) + \left(\mathbf{u}^{(k)}\right)^T\mathbf{u} - \left(\mathbf{u}^{(k)}\right)^T\mathbf{u}^{(k)} \geqslant \mathbf{1}, \tag{49e}$$

where $\nabla f\left(\mathbf{u}^{(k)}\right)$ is the gradient of $f(\mathbf{u})$ at $\mathbf{u}^{(k)}$, which can be referred to [27] (page 237) as

$$\begin{aligned}\nabla f\left(\mathbf{u}^{(k)}\right) &= \frac{2\Lambda_i\left(\mathbf{u}^{(k)}\right)^T}{\mathbf{b}_i\mathbf{u}\varsigma^2+1} - \frac{\left(\mathbf{u}^{(k)}\right)^T\Lambda_i\mathbf{u}^{(k)}}{\left(\mathbf{b}_i\mathbf{u}\varsigma^2+1\right)^2}\mathbf{b}_i \\ &= 2\Lambda_i G_i^{-1}\left(\mathbf{u}^{(k)}\right)^T - \left(\mathbf{u}^{(k)}\right)^T\Lambda_i\mathbf{u}^{(k)}G_i^{-2}\mathbf{b}_i.\end{aligned} \tag{50}$$

The optimization problem (P9) can be solved in a similar manner as in Algorithm 1 by the CVX optimization package [22]. However, due to the consideration of the signal dependent noise in conjunction with the approximation procedures, only a local solution can be found for (P9), instead of global solution in (P6). This is clearly shown in Fig. 14, where the channel capacity of both schemes are presented for a 4-LED scenario in various locations with $\varsigma^2 = 20$. In comparison with the case of $\varsigma^2 = 0$ in Fig. 11, the performance of both conventional scheme and proposed PD orientation significantly degrade. However, in various locations, the proposed scheme still maintains some capacity gaps over the conventional scheme.

VI. CONCLUSION

In this paper, we propose the optimized orientation of the PD in an SM VLC system to improve the BER performance and the unbounded channel capacity. By expressing the channel coefficient as the function of the normal vector of the PD and solving the two optimization problems, the optimal orientation of the PD can be realized. The simulation results indicate that our proposed methods obtain better error performance and a higher channel capacity in comparison with conventional SM VLC systems. For future research, we will focus on extending the result to a VLC system with multiple PDs where the condition of the channel matrix is considered and can be improved by changing the normal vectors of the PDs. Moreover, in various practical VLC systems, sometime a significant amount of received power through reflection of light can not be ignored and should be considered in the optimization problems. The PD orientation with the consideration of NLOS links evokes the issue of complexity and mobility of the receiver that will be future research.

APPENDIX

A. PROOF OF RANK ONE SOLUTION OF (P6)

Proof: The Lagrangian for problem (P6) is

$$\begin{aligned}\mathcal{L} = &\frac{1}{N_t}\sum_{j=1}^{N_t}\log\left[1+\text{tr}\left(\mathbf{G}_j\mathbf{W}\right)\right] + \sum_{j=1}^{N_t}\lambda_j\left[\text{tr}\left(\hat{\mathbf{V}}_j\mathbf{W}\right)-1\right] \\ &+\sum_{j=1}^{N_t}\mu_j\left[\cos^2\theta_{\text{fov}} - \text{tr}\left(\hat{\mathbf{V}}_j\mathbf{W}\right)\right] + \varepsilon\left[\text{tr}\left(\mathbf{W}\right)-1\right] \\ &-\text{tr}\left(\mathbf{\Lambda}\mathbf{W}\right),\end{aligned} \tag{51}$$

where $\lambda_j \geqslant 0, \mu_j \geqslant 0, \varepsilon \geqslant 0, \mathbf{\Lambda} \succcurlyeq 0$ are Lagrange multipliers for constraints (40b), (40c), (40d), and (40e) respectively. In here, $\mathbf{\Lambda}$ is a 3×3 matrix. Taking the derivative with respect to $\mathbf{W}$ we have

$$\begin{aligned}\frac{\partial\mathcal{L}}{\partial\mathbf{W}} = &\frac{1}{N_t}\sum_{j=1}^{N_t}\left[\left(1+\text{tr}\left(\mathbf{G}_j\mathbf{W}\right)\right)^{-1}\mathbf{G}_j\right] \\ &+\sum_{j=1}^{N_t}\lambda_j\hat{\mathbf{V}}_j - \sum_{j=1}^{N_t}\mu_j\hat{\mathbf{V}}_j + \varepsilon - \mathbf{\Lambda}.\end{aligned} \tag{52}$$

With an optimal solution $\mathbf{W}^*$ then we have

$$\frac{\partial \mathcal{L}}{\partial \mathbf{W}^*} = 0, \tag{53}$$

and

$$\mathbf{\Lambda}\mathbf{W}^* = 0. \tag{54}$$

From (53) and (54) we have

$$\mathbf{\Lambda} = \frac{1}{N_t}\sum_{j=1}^{N_t}\left[\left(1+\mathrm{tr}\left(\mathbf{G}_j\mathbf{W}^*\right)\right)^{-1}\mathbf{G}_j\right] + \sum_{j=1}^{N_t}\left(\lambda_j - \mu_j\right)\hat{\mathbf{V}}_j + \varepsilon. \tag{55}$$

Since $\mathrm{rank}\left(\hat{\mathbf{V}}_j\right) = 1$, the two last terms in (55) construct a full rank matrix. Moreover, recalling that $h_j = \mathbf{t}_j^T\hat{\mathbf{u}} \geqslant 0$, therefore $\left(1+\mathrm{tr}\left(\mathbf{G}_j\mathbf{W}^*\right)\right)^{-1} \geqslant 0$. Combining with $\mathrm{rank}\left(\mathbf{G}_j\right) = 1$, from (55), we can conclude that

$$\mathrm{rank}\left(\mathbf{\Lambda}\right) = 3 - 1 = 2. \tag{56}$$

Further, combing (54) and (56), we can obtain $\mathrm{rank}\left(\mathbf{W}^*\right) = 1$. This completes the proof. ■

REFERENCES

[1] M. Z. Chowdhury, M. T. Hossan, A. Islam, and Y. M. Jang, "A comparative survey of optical wireless technologies: Architectures and applications," *IEEE Access*, vol. 6, pp. 9819–9840, 2018.

[2] S. S. Bawazir, P. C. Sofotasios, S. Muhaidat, Y. Al-Hammadi, and G. K. Karagiannidis, "Multiple access for visible light communications: Research challenges and future trends," *IEEE Access*, vol. 6, pp. 26167–26174, 2018.

[3] T. Komine and M. Nakagawa, "Fundamental analysis for visible-light communication system using LED lights," *IEEE Trans. Consum. Electron.*, vol. 50, no. 1, pp. 100–107, Feb. 2004.

[4] T. Fath and H. Haas, "Performance comparison of MIMO techniques for optical wireless communications in indoor environments," *IEEE Trans. Commun.*, vol. 61, no. 2, pp. 733–742, Feb. 2013.

[5] Y.-Y. Zhang, H.-Y. Yu, and J.-K. Zhang, "Block precoding for peak-limited MISO broadcast VLC: Constellation-optimal structure and addition-unique designs," *IEEE J. Sel. Areas Commun.*, vol. 36, no. 1, pp. 78–90, Jan. 2018.

[6] A. Agarwal and S. K. Mohammed, "Achievable rate region of the zero-forcing precoder in a 2 × 2 MU-MISO broadcast VLC channel with per-LED peak power constraint and dimming control," *J. Lightw. Technol.*, vol. 35, no. 19, pp. 4168–4194, Oct. 1, 2017.

[7] Y.-Y. Zhang, "Intrinsic robustness of MISO visible light communications: Partial CSIT can be as useful as perfect one," *IEEE Trans. Commun.*, vol. 67, no. 2, pp. 1297–1312, Feb. 2019.

[8] S. Sugiura, T. Ishihara, and M. Nakao, "State-of-the-art design of index modulation in the space, time, and frequency domains: Benefits and fundamental limitations," *IEEE Access*, vol. 5, pp. 21774–21790, 2017.

[9] J. Jeganathan, A. Ghrayeb, L. Szczecinski, and A. Ceron, "Space shift keying modulation for MIMO channels," *IEEE Trans. Wireless Commun.*, vol. 8, no. 7, pp. 3692–3703, Jul. 2009.

[10] J.-Y. Wang, H. Ge, J.-X. Zhu, J.-B. Wang, J. Dai, and M. Lin, "Adaptive spatial modulation for visible light communications with an arbitrary number of transmitters," *IEEE Access*, vol. 6, pp. 37108–37123, 2018.

[11] M. L. Tran and S. Kim, "Novel bit mapping for generalized spatial modulation in VLC systems," *IEEE Photon. Technol. Lett.*, vol. 31, no. 15, pp. 1257–1260, Aug. 1, 2019.

[12] Y. S. Eroğlu, Y. Yapıcı, and I. Güvenç, "Impact of random receiver orientation on visible light communications channel," *IEEE Trans. Commun.*, vol. 67, no. 2, pp. 1313–1325, Feb. 2019.

[13] S. Arnon, Ed., *Visible light communication*. Cambridge, U.K.: Cambridge Univ. Press, 2015, p. 210.

[14] A. Nuwanpriya, S.-W. Ho, and C. S. Chen, "Indoor MIMO visible light communications: Novel angle diversity receivers for mobile users," *IEEE J. Sel. Areas Commun.*, vol. 33, no. 9, pp. 1780–1792, Sep. 2015.

[15] M. D. Soltani, H. Kazemi, M. Safari, and H. Haas, "Handover modeling for indoor Li-Fi cellular networks: The effects of receiver mobility and rotation," in *Proc. IEEE Wireless Commun. Netw. Conf. (WCNC)*, Mar. 2017, pp. 1–6.

[16] C. L. Bas, S. Sahuguede, A. Julien-Vergonjanne, A. Behlouli, P. Combeau, and L. Aveneau, "Impact of receiver orientation and position on visible light communication link performance," in *Proc. 4th Int. Workshop Opt. Wireless Commun. (IWOW)*, Sep. 2015, pp. 1–5.

[17] B. Zhou, V. Lau, Q. Chen, and Y. Cao, "Simultaneous positioning and orientating for visible light communications: Algorithm design and performance analysis," *IEEE Trans. Veh. Technol.*, vol. 67, no. 12, pp. 11790–11804, Dec. 2018.

[18] C. Masouros, "Improving the diversity of spatial modulation in MISO channels by phase alignment," *IEEE Commun. Lett.*, vol. 18, no. 5, pp. 729–732, May 2014.

[19] Z. Ghassemlooy, L. N. Alves, S. Zvanovec, and M.-A. Khalighi, *Visible Light Communications: Theory and Applications*, 1st ed. Boca Raton, FL, USA: CRC Press, 2017.

[20] S. Boyd and L. Vandenberghe, *Convex Optimization*. Cambridge, U.K.: Cambridge Univ. Press, 2004.

[21] Z.-Q. Luo, W.-K. Ma, A. M.-C. So, Y. Ye, and S. Zhang, "Semidefinite relaxation of quadratic optimization problems," *IEEE Signal Process. Mag.*, vol. 27, no. 3, pp. 20–34, May 2010.

[22] (Sep. 2013). *CVX: MATLAB Software for Disciplined Convex Programming*. [Online]. Available: http://cvxr.com/cvx

[23] E. A. Rakhmanov, E. B. Saff, and Y. M. Zhou, "Minimal discrete energy on the sphere," *Math. Res. Lett.*, vol. 1, no. 6, pp. 647–662, Nov. 1994.

[24] S. Sugiura and H. Iizuka, "Element-by-element full-rank optical wireless MIMO systems using narrow-window angular filter designed based on one-dimensional photonic crystal," *J. Lightw. Technol.*, vol. 34, no. 24, pp. 5601–5609, Dec. 15, 2016.

[25] Q. Gao, S. Hu, C. Gong, E. Serpedin, K. Qaraqe, and Z. Xu, "Distance-range-oriented constellation design for VLC-SCMA downlink with signal-dependent noise," *IEEE Commun. Lett.*, vol. 23, no. 3, pp. 434–437, Mar. 2019.

[26] S. Hu, Q. Gao, C. Gong, Z. Xu, R. Boluda-Ruiz, and K. Qaraqe, "Energy-efficient modulation for visible light SCMA system with signal-dependent noise," in *Proc. 11th Int. Symp. Commun. Syst., Netw. Digit. Signal Process. (CSNDSP)*, Jul. 2018, pp. 1–6.

[27] S. Boyd and L. Vandenberghe, *Convex Optimization*. Cambridge, U.K.: Cambridge Univ. Press, 2006.

MANH LE TRAN received the B.S. degree from the Posts and Telecommunications Institute of Technology, in 2015. He is currently pursuing the M.S./Ph.D. combined program as a Researcher with the School of Electrical Engineering, University of Ulsan, South Korea. He was a Mobile Network Engineer with the Viettel Group, Vietnam, from 2015 to 2016. His main research interests include 5G communication, visible light communications, and signal processing.

SUNGHWAN KIM received the B.S., M.S., and Ph.D. degrees from Seoul National University, South Korea, in 1999, 2001, and 2005, respectively. He was a Postdoctoral Visitor with the Georgia Institute of Technology (GeorgiaTech), from 2005 to 2007, and a Senior Engineer with Samsung Electronics, from 2007 to 2011. He is currently a Professor with the School of Electrical Engineering, University of Ulsan, South Korea. His main research interests include channel coding, modulation, massive MIMO, visible light communication, and quantum information.